Shared Steering Control Between a Driver and an Automation: Stability in the Presence of Driver Behavior Uncertainty

Louay Saleh, Philippe Chevrel, Fabien Claveau, Jean-François Lafay, and Franck Mars

***Abstract*—This paper presents an advanced driver assistance system (ADAS) for lane keeping, together with an analysis of its performance and stability with respect to variations in driver behavior. The automotive ADAS proposed is designed to share control of the steering wheel with the driver in the best possible way. Its development was derived from an H2-Preview optimization control problem, which is based on a global driver–vehicle–road (DVR) system. The DVR model makes use of a cybernetic driver model to take into account any driver–vehicle interactions. Such a formulation allows 1) considering driver assistance cooperation criteria in the control synthesis, 2) improving the performance of the assistance as a cooperative copilot, and 3) analyzing the stability of the whole system in the presence of driver model uncertainty. The results have been experimentally validated with one participant using a fixed-base driving simulator. The developed assistance system improved lane-keeping performance and reduced the risk of a lane departure accident. Good results were obtained using several criteria for human–machine cooperation. Poor stability situations were successfully avoided due to the robustness of the whole system, in spite of a large range of driver model uncertainty.**

***Index Terms*—Driver model, H2-Preview, lane keeping, shared steering control, vehicle lateral control.**

I. Introduction

DRIVING is a dangerous activity that can have serious human and economic consequences. According to the statistics, unintended lane departure is the second most frequent type of single light-vehicle accidents [1]. In many cases, the accidents can be attributed to degradation in driver performance, which is caused by such factors as fatigue, drowsiness, or inattention. This fact has motivated major research effort aimed at helping drivers and improving safety, particularly through the use of active systems that have the potential to prevent vehicle accidents.

Several advanced assistance systems have been proposed over the last decade to improve vehicle lateral control [2]. Some of them are based on the principle of mutual control between the driver and the automation system. The challenge in designing such human–machine interaction is how to combine the adaptability of humans with the precision of machines because manual control tasks are prone to human error, and fully automated tasks are subject to wide-ranging limitations. Recently, an alternative solution, known as haptic shared control or haptic guidance [3], has received increased attention. In the shared control paradigm, the machine's manual control interface is motorized to allow both a human and a controller to be able to exert control simultaneously [4]. In such a setup, the haptic interface can sense the action of the operator and feed the forces back to him. Shared control has been investigated for a wide range of applications, e.g., in the control of automobiles [5], [6], and aircraft [7], or during tele-operated control to support object manipulation [8], surgery [9], microassembly [10], or the steering of unmanned aerial vehicles [11].

Haptic feedback on the steering wheel is reported in the literature as a promising way to support drivers during a steering task [4]. One successful realization is the lane-keeping assistance system (LKS), which continuously produces torque on the steering wheel to match predicted lateral lane deviations (e.g., in the 2001 Nissan Cima and the 2004 Honda Accord). Thus, both the driver and the support system contribute to the steering task. The benefit is that the driver is aware of the system's actions and can choose to overrule them.

Such LKS systems are often designed based on a vehicle–road (VR) model and consider driver action as a disturbing signal. Therefore, these systems do not guarantee the global stability of driving and cannot provide a robustness analysis in the presence of variations in driver's behavior. A performance analysis of LKS systems has highlighted the fact that the vehicle and the driver form a human–machine system. Such a system should be considered as a whole to develop a cooperative co-pilot that monitors the driver's control actions, and understands and corrects them if necessary. For this reason, a cybernetic approach is recommended for modeling any interactions between drivers and the vehicle environment [12].

This paper proposes haptic guidance that is based on the concept of shared control, where both the driver and the

Manuscript received August 28, 2012; revised December 17, 2012; accepted February 14, 2013. Date of publication March 19, 2013; date of current version May 29, 2013. This work was supported by the Agence Nationale de la Recherche through the National Project PARTAGE under Grant ANR 0866C0222. The Associate Editor for this paper was C. Wu.

L. Saleh was with IRCCyN UMR CNRS 6597 (Institut de Recherche en Communications et Cybernétique de Nantes), 44321 Nantes, France. He is now with the Higher Institute of Applied Sciences and Technology, Damascus 31983, Syria (e-mail: louaysaleh@gmail.com).

P. Chevrel, F. Claveau, J.-F. Lafay, and F. Mars are with the LUNAM Université, Ecole des Mines de Nantes, Ecole Centrale de Nantes, CNRS, IRCCyN UMR CNRS 6597 (Institut de Recherche en Communications et Cybernétique de Nantes), 44321 Nantes, France (e-mail: philippe.chevrel@mines-nantes.fr; fabien.claveau@irccyn.ec-nantes.fr; jean-francois.lafay@irccyn.ec-nantes.fr; franck.mars@irccyn.ec-nantes.fr).

Color versions of one or more of the figures in this paper are available online at http://ieeexplore.ieee.org.

Digital Object Identifier 10.1109/TITS.2013.2248363

1524-9050/$31.00 © 2013 IEEE

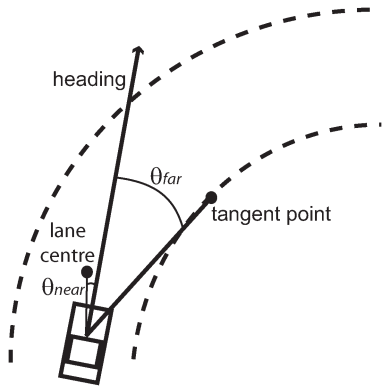

Fig. 1. Near and far visual points.

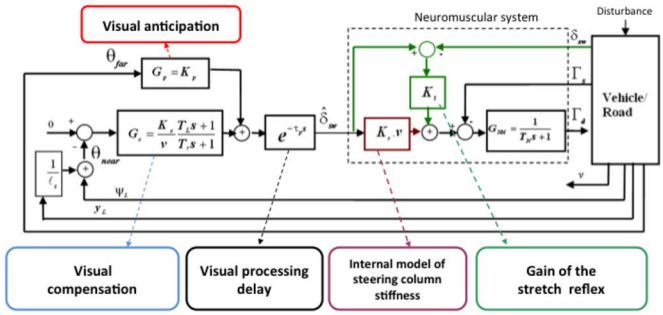

Fig. 2. Cybernetic driver model for lane keeping.

guidance system act on the steering wheel. The shared control is built over a closed-loop driver–vehicle–road (DVR) model. In Section II, a traditional VR model is combined with a newly developed cybernetic driver model to formulate the closed-loop DVR model. Section III shows a shared control law that is based on the H2-Preview control approach. It is then experimentally evaluated in terms of safety improvement and cooperation with the driver. In Section IV, robustness against driver model uncertainties is studied using μ-analysis.

II. Closed-Loop Driver–Vehicle–Road Model

A. Driver Model

A cybernetic driver model for vehicle lateral control that takes into account what is known about sensorimotor and cognitive control in humans has recently been proposed in [13] and [14]. The model was identified and validated using experiments with human drivers on SCANeR, which is a fixed-base driving simulator. Here, we briefly present the essential information on the driver model in the perspective of designing the shared control law. A more detailed presentation of the model psychophysiological background can be found in [13]. (For more details about driver modeling, identification, and validation, see [14].)

The developed model is based on the hypothesis that drivers use visual information to identify the approaching road curvature and the position of the vehicle in relation to the edge lines. Drivers have been shown to use "near" and "far" vision of the roadway for steering, which is represented in a model by the angles between the car heading and two distinct points [15]. The near point is used to maintain a central lane position; it is assumed to be at a convenient distance from the front of the vehicle. It is near enough to monitor lateral position but far away enough to be seen through the vehicle windshield (look-ahead distance l_s, fixed here at 5 m). The far point is used to account for the upcoming roadway curvature. It is assumed to be the tangent point, i.e., the point where the direction of the inside edge line seems to reverse from the driver's viewpoint (see Fig. 1).

Based only on visual observations, the steering task is considered a tracking task with compensatory and anticipatory components (see Fig. 2). The compensatory part G_c exploits near angle θ_{near}, which represents the relative placement of the vehicle compared with the lane center. The anticipatory part G_p, by which the driver compensates the road curvature, uses far angle θ_{far}, which is the angle between the car heading and the tangent point. At the output of both these components, the driver formulates some kind of intention, which is considered the desired steering angle Δ_{sw}.

TABLE I
Driver Model Parameters

	Parameter rule	Nominal value	Variation interval
K_p	Anticipation gain	3.4	[2-5]
K_c	Compensation gain	15	[5-25]
T_I	Compensation lag-time constant	1	[0.5-1.5]
T_L	Compensation lead-time constant	3	[2-4]
τ_p	Processing time delay	0.03	[0-0.06]
K_r	Angle to torque coefficient	0.3	[0.2-0.4]
K_t	Neuromuscular reflex gain	0.5	[0-1]
T_N	Neuromuscular time constant	0.1	

Some time delay τ_p is assumed for processing visual information into an intention of action. Here, the driver's intention is converted into the torque command Γ_d by means of the neuromuscular system (NMS). The NMS is modeled according to [16], although alternatives exist [17], [18]. It includes feedforward action G_r and a closed-loop reflex gain K_t. G_r represents the internalized angle-to-torque stiffness characterizing the steering column. K_t represents the neuromuscular reflex that rejects any disturbance torque on the steering wheel that is caused by an external disturbance such as a gust of wind. This gain continuously acts to minimize the difference $\Delta\delta$ between the measured steering angle δ_d and the desired one δ_{sw}. G_{NM} is a simplified model of arm dynamics. The proposed driver model supposes that the driver applies torque Γ_d to the steering wheel, taking into account the self-aligning torque Γ_s and the eventual assistance torque Γ_a. The developed driver model is adjusted by the longitudinal speed V_x.

The adopted cybernetic approach has highlighted the relations between the model parameters and the perceptual and motor abilities of the human driver. The eight parameters of the model (summarized in Table I) have been estimated using the prediction error method [19]. The estimation was carried out using measurements from experiments that involved five human drivers who drove along a test track in a driving simulator that uses SCANeR software (see Fig. 7). The model was then validated using the identified model to drive the simulator. The results indicate that the proposed model matches driver

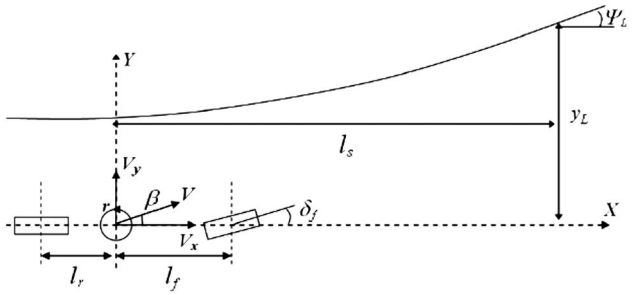

Fig. 3. VR model for lane keeping.

steering with a fit of 70% on average, which is a satisfying performance considering the large intra-individual and inter-individual variability in steering behavior. The model also provided a reasonably accurate prediction of the driver's action for the design of the shared control law.

Table I shows the nominal values of parameters obtained for one of the participants in the experiments and an estimated domain of variation for each parameter. This variation domain has been estimated using the results of the identification procedure performed on the experimental data obtained in this paper.

The driver state-space model can be derived in Fig. 2. A minimal representation is given by

$$\begin{bmatrix} \dot{x}_{1d} \\ \dot{x}_{2d} \\ \dot{\Gamma}_d \end{bmatrix} = \begin{bmatrix} a_{11d} & 0 & 0 \\ a_{21d} & a_{22d} & 0 \\ a_{31d} & a_{32d} & a_{33d} \end{bmatrix} \begin{bmatrix} x_{1d} \\ x_{2d} \\ \Gamma_d \end{bmatrix} + \begin{bmatrix} 0 & b_{12d} & 0 & 0 \\ b_{21d} & b_{22d} & 0 & 0 \\ b_{31d} & b_{32d} & b_{33d} & b_{34d} \end{bmatrix} \begin{bmatrix} \theta_{\text{for}} \\ \theta_{\text{near}} \\ \delta_d \\ \Gamma_s - \Gamma_a \end{bmatrix}$$

$$\Gamma_d = \begin{bmatrix} 0 & 0 & 1 \end{bmatrix} \begin{bmatrix} x_{1d} \\ x_{2d} \\ \Gamma_d \end{bmatrix}. \quad (1)$$

The matrices coefficients in (1) are linked to the driver model parameters, as given in the Appendix. State x_{1d} is linked to block "G_c" in Fig. 2 and can be interpreted as the driver's perception of the steering-wheel adjustment to be done in the near future by considering the θ_{near} angle variation. x_{2d} is the state of the first-order Pade approximation of the delay block $e^{-\tau_p s}$ leading to signal δ_{sw}. By itself, it is a good indicator (in low frequencies) of the driver steering intention.

B. VR Model

The general VR model considered here for lateral control involves the dynamics of the lane-keeping visual process, the steering column, and the lateral vehicle dynamics. According to [20], The VR model can be written as

$$\dot{x}_{\text{VR}} = A_{\text{VR}} x_{\text{VR}} + B_{1\text{VR}}(\Gamma_a + \Gamma_d) + B_{2\text{VR}}\, \rho_{\text{ref}}$$
$$A_{\text{VR}} \in \Re^{6\times 1}; \quad B_{1\text{VR}} \in \Re^{6\times 1}; \quad B_{2\text{VR}} \in \Re^{6\times 1} \quad (2)$$

where $x_{\text{VR}} = [\beta,\, r,\, \psi_L,\, y_L,\, \delta_d,\, d\delta_d/dt]^T$ is the VR state vector. It consists of (see Fig. 3) the following: side slip angle β, yaw rate r, heading angle ψ_L, the offset from the lane center y_L projected forward on the look-ahead distance l_s, steering angle δ_d, and steering speed $d\delta_d/dt$.

TABLE II
PEUGEOT 307 MODEL PARAMETERS

l_f	distance form Gravity Center to front axle	1.127 m
l_r	distance from Gravity Center to rear axle	1.485 m
M	total mass	1476 Kg
J	vehicle yaw moment of inertia	1810 Kg.m^2
C_{f0}	front cornering stiffness	65000 N/rad
C_{r0}	rear cornering stiffness	57000 N/rad
η_t	tire length contact	0.185 m
μ	adhesion	0.8
K_m	manual steering column coefficient	1
R_S	steering gear ratio	16
B_s	Steering system damping coefficient	5.73
I_s	inertial moment of steering system	0.05 Kg.m^2
l_s	look-ahead distance	5 m

The inputs of (2) are steering torque command $\Gamma_a + \Gamma_d$ and road curvature ρ_{ref}. Matrices A_{VR}, $B_{1\text{VR}}$, and $B_{2\text{VR}}$ are given by

$$A_{\text{VR}} = \begin{bmatrix} a_{11c} & a_{12c} & 0 & 0 & a_{15c} & 0 \\ a_{21c} & a_{22c} & 0 & 0 & a_{25c} & 0 \\ 0 & 1 & 0 & 0 & 0 & 0 \\ V_x & l_s & V_x & 0 & 0 & 0 \\ 0 & 0 & 0 & 0 & 0 & 1 \\ \frac{T_{S\beta}}{I_s} & \frac{T_{Sr}}{I_s} & 0 & 0 & -\frac{T_{S\beta}}{R_S I_s} & -\frac{B_s}{I_s} \end{bmatrix}$$

$$B_{1\text{VR}} = \begin{bmatrix} 0 & 0 & 0 & 0 & 0 & \dfrac{I}{I_s} \end{bmatrix}^T$$

$$B_{2\text{VR}} = \begin{bmatrix} 0 & 0 & -V_x & -l_s V_x & 0 & 0 \end{bmatrix}^T.$$

The values of matrix coefficients are given in the Appendix. VR parameters are summarized in Table II with nominal values that correspond to a Peugeot 307 car. This vehicle model was used on the driving simulator to identify the driver model (see Table I). It will support the shared lateral control synthesis in Section III.

C. Global DVR Model

The DVR model can be deduced from aggregation of the models (1) and (2) as

$$\dot{x} = Ax + B_1\Gamma_a + B_2\, \rho_{\text{ref}},$$
$$A \in \Re^{9\times 9}; \quad B_1 \in \Re^{9\times 1}; \quad B_2 \in \Re^{9\times 1} \quad (3)$$

where $x = [x_{\text{VR}},\, x_{1d},\, x_{2d},\, \Gamma_d]$ is the DVR state vector. The matrices A, B_1, and B_2 are shown at the bottom of the next page. The coefficients of these matrices (given in the Appendix) are determined as a function of the VR (see Table II) and driver model parameters (see Table I).

Setting up the DVR model is carried out by considering some slight approximations. The near angle is written as $\theta_{\text{near}} \approx \psi_L + y_L/l_s$, and the far angle is approximated as

$\theta_{\text{far}} \approx D_{\text{far}} \times \rho_{\text{ref}}$, where D_{far} is the distance to the tangent point. These approximations have been analyzed and validated during this study.

III. Lateral Shared Control

A. Performance Assessment

The evaluation of control performance usually involves a tradeoff between multiple and potential conflicting criteria. Steering assistance systems should assist the driver in keeping the vehicle within the lane and thus contribute to active safety. At the same time, the assistance system should cooperate with the driver and avoid conflict with him as much as possible. In the absence of standards to evaluate the performance of new systems, compared with existing ones, we will define different indicators that allow the measurement of what is deemed as "safe driving" and a "cooperative co-pilot." Some are commonly used metrics for lane-keeping performance, whereas others are innovative.

One of the most common metrics for lane-position performance evaluation is lateral deviation error. In particular, we chose to examine the mean absolute lateral deviation from the centerline and the standard deviation of lateral position. These indicators do not permit the evaluation of the lane departure risk (LDR), but the well-known time to lane crossing (TLC) does. TLC is defined as the time available for a driver until any part of the vehicle reaches one of the lane boundaries [21]. There are several ways of computing TLC values with more or less approximation of the road curvature and trajectory prediction [22]. Here, the TLC, named the TLC path (TLCP), was estimated by assuming that the vehicle yaw rate and heading speed were maintained as constant in the near future (see Fig. 4). The advantage of TLCP is that it is less sensitive to transient steering deviations because they are filtered by vehicle dynamics.

Since the risk of lane departure is also driver dependent, TLCP alone cannot provide a consistent evaluation, particularly when the driver intentionally cuts bends or when he is aware of the risk and has already acted to correct it. In these two cases, TLCP overestimates the risk as it does not take into account the driver's intention. To overcome this deficiency, the proposition here is to estimate the driver's steering intention

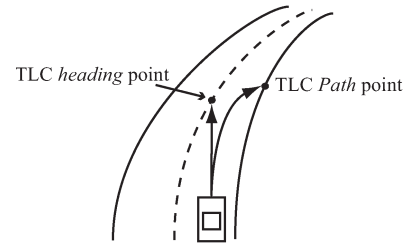

Fig. 4. Path and heading time to line crossing.

through the cybernetic model previously introduced (see the internal variable δ_{sw}). The *driving error* $\Delta\delta$ is then defined as the deviation of the actual driver steering angle from δ_{sw}, which is the angle predicted by the driver reference model.

We propose evaluating the risk of lane departure through the following LDR criteria:

$$\text{LDR} = \frac{\Delta\delta}{\text{TLCP}}.$$

The LDR value is normalized within a [0–1] risk interval. As long as the LDR indicates a low threat level, the driving is "safe."

On the other hand, the cooperative performance of a given (electronic) co-pilot will be evaluated using the following criteria:

- consistency rate T_{co}, which is defined as the ratio of the period during which the assistance torque Γ_a is in the same direction as the driver torque (Γ_d), divided by the total driving period;
- resistance rate T_{res}, which is defined as the ratio of the period during which Γ_a is in the opposite direction to Γ_d but Γ_a is inferior to Γ_d, divided by the total driving period;
- contradiction rate T_{cont}, which is defined as the ratio of the period during which Γ_a overcomes Γ_d, divided by the total driving period.

In a preliminary presentation of this paper [23], we also proposed an original indicator of cooperative performance using the driver and automation torque. These two signals may be considered a member of the L2 Hilbert space, with the possibility of defining their scalar product and the angle between

$$A = \begin{bmatrix} a_{11c} & a_{12c} & 0 & 0 & a_{15c} & 0 & 0 & 0 & 0 \\ a_{21c} & a_{22c} & 0 & 0 & a_{25c} & 0 & 0 & 0 & 0 \\ 0 & 1 & 0 & 0 & 0 & 0 & 0 & 0 & 0 \\ V_x & l_s & V_x & 0 & 0 & 0 & 0 & 0 & 0 \\ 0 & 0 & 0 & 0 & 0 & 1 & 0 & 0 & 0 \\ a_{61c} & a_{62c} & 0 & 0 & a_{65c} & a_{66c} & 0 & 0 & b_{61c} \\ 0 & 0 & b_{12d} & b_{12d}/\ell_s & 0 & 0 & a_{11d} & 0 & 0 \\ 0 & 0 & b_{22d} & b_{22d}/\ell_s & 0 & 0 & a_{21d} & a_{22d} & 0 \\ b_{n31d} & b_{n32d} & b_{32d} & b_{32d}/\ell_s & b_{n35d} & 0 & a_{31d} & a_{32d} & a_{32d} \end{bmatrix}$$

$$B_1 = \begin{bmatrix} 0 & 0 & 0 & 0 & 0 & b_{61c} & 0 & 0 & -b_{34d} \end{bmatrix}^T$$

$$B_2 = \begin{bmatrix} 0 & 0 & -V_x & -V_x - l_s & 0 & 0 & 0 & b_{21d}D_{\text{for}} & b_{31d}D_{\text{for}} \end{bmatrix}^T$$

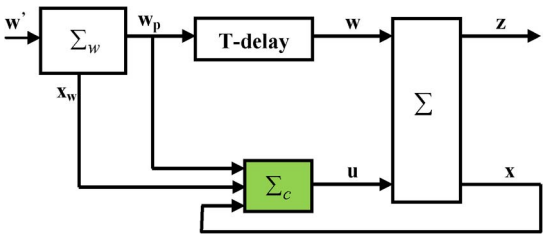

Fig. 5. H2-Preview controller problem.

them. This angle can be used to represent the contradiction level between the driver's action and that of the automated device.

B. Preview-Based Controller Design

The assistance strategy is developed by applying the H2-Preview control approach described in [20] to the global DVR model. Such a control design is known to guarantee improved performance when the near future of the exogenous signal, in this case the road curvature, is known.

Consider the linear time-invariant system Σ as follows:

$$\begin{aligned} \dot{x} &= Ax + B_1 u + B_2 w \\ z &= Cx + D_1 u, \\ & A \in \Re^{n\times n}; \quad B_1 \in \Re^{n\times m}; \quad B_2 \in \Re^{n\times r} \\ & C \in \Re^{p\times n}; \quad D_1 \in \Re^{p\times m} \end{aligned} \tag{4}$$

where x is the state vector, u the control input, w the disturbance input, and z the performance vector output. The "optimal H2-Preview controller problem" [20], [24], [25] is defined as the problem of finding controller Σ_c that rejects the effect of the input disturbances w (known in advance over time T) on output z (see Fig. 5). The controller has to stabilize the closed-loop system of Fig. 5 and minimize the performance H2 index (5) under the assumption that the previewed exogenous input $w_p(t) = w(t+T)$ is correctly modeled, beyond the preview horizon, through the generator model Σ_w described by (6), where w' is an unpredictable signal, as shown in the following:

$$J = \|z\|_2^2 = \int_0^\infty z^T(t) z(t) dt \tag{5}$$

$$\begin{aligned} \dot{x}_w &= A_w x_w + B_w w \\ w_p &= C_w x_w \\ & A_w \in \Re^{q\times q}; \quad C_w \in \Re^{r\times q}; \quad B_w \in \Re^{q\times q}. \end{aligned} \tag{6}$$

Theorem 1: Let system (Σ, Σ_w) be defined by (4) and (6). Assume the following.

- Pair (A, B_1) can be stabilized.
- Quadruple (A, B_1, C, D_1) has no invariant zeroes on.
- D_1 is a full-column rank matrix.
- A_w is Hurwitz.

Let $R = D_1^T D_1$, $Q = C^T C$, and $S = C^T D_1$. The solution of the H2-preview problem is given by controller Σ_c defined through the following relation:

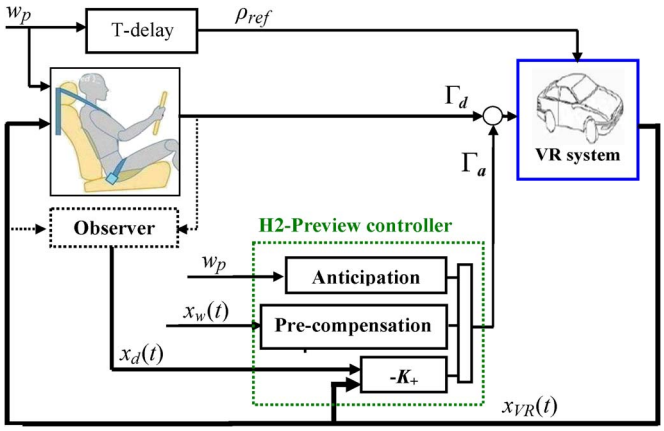

Fig. 6. H2-Preview shared control.

$$u(t) = -K_+ x(t) + \int_0^\infty \Phi(\tau) w_p(t-\tau) d\tau - R^{-1} B_1^T e^{A_+^T T} M x_w(t) \tag{7}$$

where

- $K_+ = R^{-1}(S^T + B_1^T P_+)$ is the gain feedback matrix.
- $\Phi(\tau) = -R^{-1} B_1^T e^{A_+^T(T-\tau)} P_+ B_2$, P_+ is the stabilizing solution of the algebraic Riccati equation, i.e., $PA + A^T P - (S + PB_1)R^{-1}(S^T + B_1^T P) + Q = 0$.
- $A_+ = A - BR^{-1}(S^T + B^T P_+)$ is the closed-loop matrix.
- M is the solution of the Sylvester equation, i.e., $A_+^T M + M \cdot A_w + P_+ B_2 C_w = 0$.

For the proof, see [20].

Based on the H2-Preview approach, the synthesis of the assistance controller is performed in continuous time to minimize the performance H2 index (5), where z is a performance vector that contains signals correlated with road tracking quality (e.g., heading angle error ψ_L), lane-keeping quality (e.g., lateral deviation y_L), control effort (e.g., assistance torque Γ_a), driver assistance sharing, and cooperation quality (e.g., $\Gamma_a - \Gamma_d$ and the scalar product $\Gamma_a \times \Gamma_d$ whose value depends on the cosine of the angle between the two torque values; this angle represents the contradiction between the driver and the automation).

Two comments should be added. First, the assumptions of Theorem 1 are all satisfied; in particular, the A_w matrix of the road curvature model is stable (Hurwitz). Indeed, this signal has a zero mean value and may be truncated in sequences of asymptotically convergent signals. Second, the introduction of "cooperation" criteria in the vector z is made possible due to the driver model.

Finally, the obtained optimal preview shared control consists of three terms (Fig. 6):

- a state-feedback term $-K_+ x$;
- an anticipation term elaborated through a finite impulse response (FIR) filter from the previewed curvature signal w_p on the preview horizon T;
- a precompensation term, which copes with the predicted road curvature beyond the preview horizon. The predictor system Σ_w is chosen to focus on the frequency interval [0–20] rad/s, which is realistic.

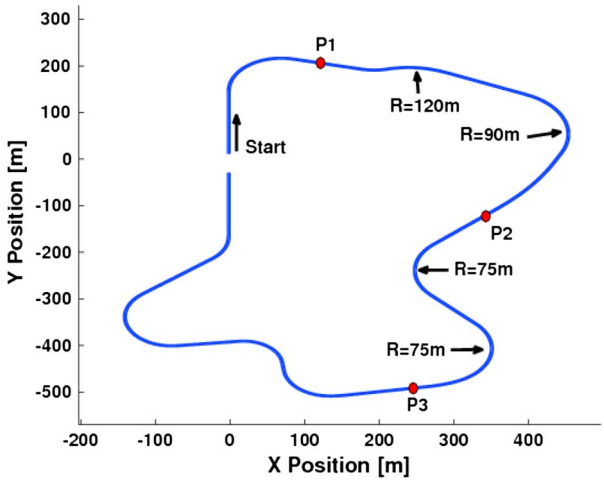

Fig. 7. Test track used in the simulator study.

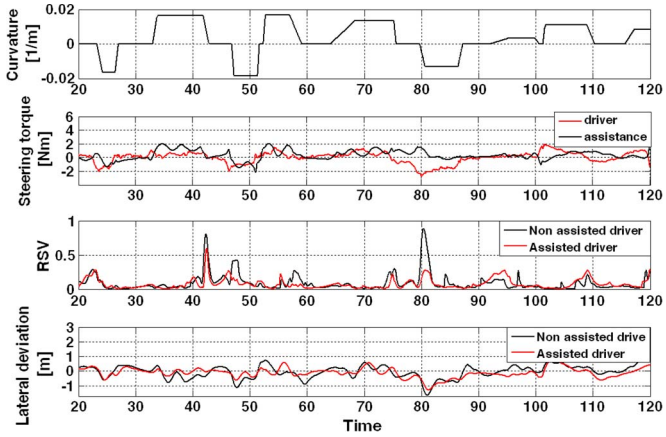

Fig. 8. Experimental evaluation results.

The H2 control may have different interpretations, one of them being the linear-quadratic-Gaussian control. In the context of this paper, the road curvature is assumed to be colored noise, with a zero mean value and a restricted bandwidth. This is compatible with the signal model used and is incorporated with the H2 standard model supporting the H2 control synthesis. This H2 criterion was preferred to the H_∞ criterion because it may be easily split into elementary H2 criteria associated with each individual control objectives. Moreover, we considered that it made more sense to work with the most probable road trajectories, than considering the worst case of road curvature only.

Let us recall that the H2 optimization problem is now a classical problem [26]. Its analytic solution may be deduced from solving Riccati equations. Different algorithms exist to solve efficiently such an equation (hence, computing the feedback gain $K+$). The only originality of our approach (see [20]), as far as optimization is concerned, is the way to deal with the disturbing signal $w(t)$, by considering both a dynamic ad hoc model and preview information on it to perform an optimal feedforward. Once again, the optimum may be analytically obtained, partly as a continuous-time FIR filter (see Theorem 1).

Numerically, this shared control is designed to match the driver whose parameters are shown in Table I and the Peugeot 307 vehicle, characterized by Table II parameters.

C. Simulator Study

Experimental tests were carried out with one driver using a fixed-base driving simulator (SCANeR) on a virtual road track of about 2.5 km in length, which consists of several curved sections including tight bends (with radius up to 70 m, see Fig. 7). The longitudinal speed was fixed at 18 m/s (the maximum safe speed for negotiating some of the tight bends on the track). Before the test trials, the driver was trained to drive the simulator. Four test trials with the driving assistance system were interleaved with four trials without assistance. In all cases, the driver was instructed to maintain a central lane position.

TABLE III
"SAFE DRIVING" PERFORMANCE EVALUATION

	Mean (LDR)	STD (LDR)	Mean (y_{act})	STD (y_{act})
Driver without assistance	0.096	0.095	0.38m	0.31m
Driver with assistance	0.081	0.084	0.27m	0.23m
% of reduction	15.6%	11.6%	28.9%	25.8%

TABLE IV
"COOPERATIVE CO-PILOT" PERFORMANCE

T_{co}	T_{res}	T_{cont}
0.55	0.27	0.18

Fig. 8 shows the road curvature, driver and assistance torque, LDR, and lateral deviation for one assisted and one nonassisted trials.

As shown in Table III, the shared control system reduced the average and variability of lateral deviation and LDR.

As for cooperation evaluation, Table IV shows the average values for rates of consistence, resistance, and contradiction over the four trials. The assistance torque was consistent with the driver torque during 55% of the driving time; it resisted the driver torque 27% of the time, and entered into conflict with the driver only 18% of the time to correct some potentially risky situation.

Thus, this case study showed that driving with the system could markedly improve lane-keeping performance. A more extensive evaluation of human–machine cooperation issues is now required to confirm the potential of this system in terms of safety and comfort. This is discussed in Section V.

IV. ROBUSTNESS ANALYSIS IN PRESENCE OF PARAMETRIC UNCERTAINTY

The performance of a nominally stable uncertain system model will generally degrade for specific values of its uncertain parameters. Moreover, the maximum possible degradation increases as the uncertain parameters are allowed to deviate in a large interval from their nominal values.

The uncertainties about the driver model parameters could be due to the quality of identification, the variability of driver behavior, or even the variety of driving styles. The latter is

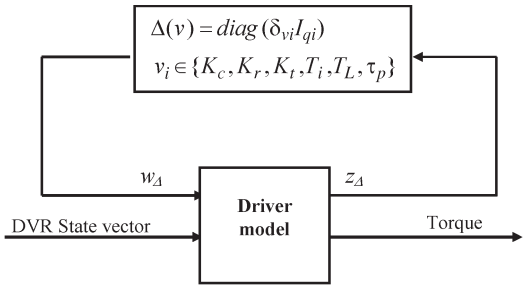

Fig. 9. Linear fractional representation of the driver model.

relevant if the assistance system is aimed at being robust enough to meet the needs of a class of drivers without adaptation.

Let us consider that the parameters characterizing the driver model are constant but uncertain. Then, the driver model can be recast using a linear fractional representation (LFR) [28] in which the uncertainties are gathered in matrix Δ, as shown in Fig. 9. The nominal driver model is then replaced by the uncertain one in the assisted closed-loop DVR system (see Fig. 6).

Each uncertain parameter is normalized and represented as

$$v = v_0 + v_1 \delta_v$$

where $\delta_v \in [-1; +1]$, (ν_0) is the nominal value, and ν_1 is the possible variation around the nominal value. The matrix Δ is diagonal and written as follows:

$$\Delta(v) = \mathrm{diag}(\delta_{vi} I_{qi}).$$

$|\delta_{vi}| < 1$ is the normalized deviation of the ith parameter of Δ. q_i is the number of repetitions of the parameter v_i in the matrix Δ. z_Δ and w_Δ are signals of appropriate dimension. The construction of the LFR model can be done numerically, e.g., by using the *ad hoc* MATLAB function "lftdata."

If the uncertain system is stable for all values of the uncertain parameters within their allowable ranges, the uncertain system is said to be robustly stable. This problem is addressed here using the structured singular-value μ-analysis [28], by considering the global system of Fig. 6 in which the nominal driver model is replaced by the uncertain one (see Fig. 9). Rather than computing the exact value of μ, which is known to be an NP complex problem, upper and lower bounds (μ_{Upper} and μ_{Lower}) on the stability margin are evaluated, using algorithms described in [29] and [30] for μ_{Lower}, and [31] and [32] for μ_{Upper}. Thus, the system is guaranteed to be stable for all modeled uncertainties with a deviation up to $1/\mu_{\mathrm{Upper}}$. From an optimistic point of view, there are no known uncertainties that question stability within the $1/\mu_{\mathrm{Lower}}$ interval. The smallest deviation $|\delta_\nu|_{\min}$ that leads to system instability may be exhibited through ad hoc programs (e.g., *mussv* of the Robust Control Toolbox of MATLAB). These use frequency-domain arguments to determine the condition leading to pole migration (due to variability of the uncertain parameters) across the imaginary axis, and the critical frequency of these poles.

Table V shows the results obtained from the μ-analysis. It shows the parameter margins within which the overall driving system is stable, and the percentage of allowable deviation for each parameter according to the original interval fixed in Table I. In addition, the worst case configuration that leads to instability is given.

TABLE V
ROBUSTNESS MARGINS

	Nominal value	Variations in the stability limits	Allowable deviation (%)	Worst-case configuration
K_c	15	[10-20]	50%	20
T_I	1	[0.8-1.5]	40%	0.8
T_L	3	[2-4]	100%	4
τ_p	0.03	[0.02-0.04]	33%	0.04
K_r	0.3	[0.25-0.35]	50%	0.35
K_t	0.5	[0.2-1.5]	60%	0.2

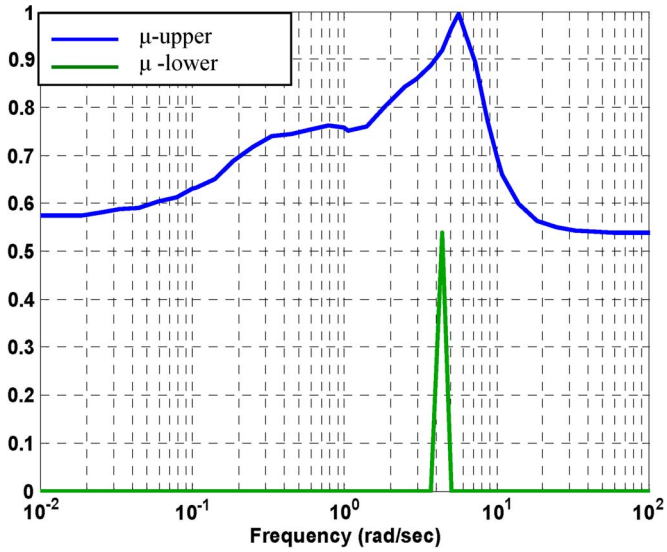

Fig. 10. μ-plot.

We note that the stability margin is particularly sensitive to the value of the processing delay for visual information. This delay should not exceed 40 ms. Table V takes a pessimistic point of view, showing that the global driving system will stay stable for a wide range of driver populations.

Fig. 10 shows μ-plot as a function of frequency. The analysis focuses on the frequency interval $w = [1 - 10]$ rad/s, which corresponds to the domain in which the shared lateral control may be critical with regard to the requirement for robustness.

Both μ upper and lower bounds converge consistently. The robustness margins found previously (see Table V) correspond to the μ upper bound. An optimistic estimation of robustness using the μ lower bound indicates that the robustness margins can be doubled while still preserving stability. This optimistic estimation covers nearly all driver populations. The worst case (Table V) scenario occurs at a frequency of 5 rad/s for a driver who:

- overcompensates the lateral deviation from the lane center (upper bound for K_c and T_L, and lower bound for T_I);
- is distracted (upper bound for processing time delay τ_p);
- is nervous (upper bound for K_r);
- loosely holds the steering wheel (lower bound for K_t).

The stability of the whole system was tested using the SCANeR driving simulator and the track shown in Fig. 7, with

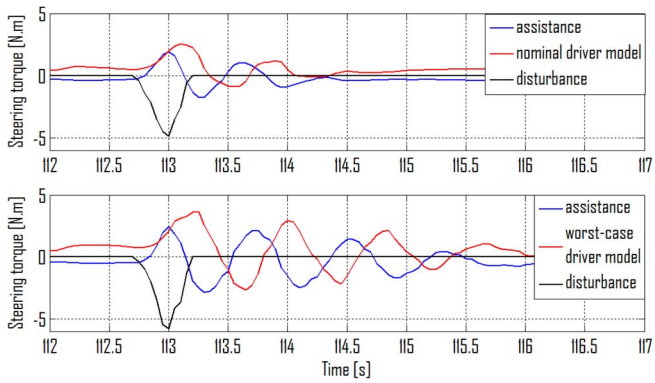

Fig. 11. Disturbance rejection with nominal case and worst case drivers.

the nominal and worst case driver models. Both experiments were carried out at a speed of $v = 65$ km/h. Fig. 11 shows the disturbance rejection performance in both cases (nominal and worst cases). Disturbance torque of about 5 N · m was applied to the steering wheel by an external source. The nominal driver model smoothly corrects the resulting errors, whereas the "worst case" models oscillate with a small damping effect, reflecting their proximity to the instability region.

The system is still stable, although it has been defined as being the worst case driver. This is because μ is estimated conservatively. In practice, we did not encounter a driver whose interactions destabilized the overall system.

However, any further comparison is not possible because of the driver's adaptation to the proposed assistance. In fact, by comparing the identified driver model to the driver behavior, it can be observed that the driver adapts his behavior, to some extent, to the steering assistance. By taking into account such driver adaptation, a new field of investigation is opened up. Further research would involve a more in-depth investigation of the stability of the overall system.

V. Conclusion and Perspectives

In summary, this paper has presented a DVR model that includes a cybernetic driver model. Based on this global model, a steering assistance system has been designed to perform shared control of the steering wheel. A simulator study showed that an improved performance lane, keeping with a low level of negative interference between the driver and the system, could be achieved. Robust stability analysis in the presence of driver model variability was also carried out. The results were compared with those achieved on the driving simulator. The performance and robustness of the proposed H2-Preview controller was shown for a large class of driver models.

Before considering the implementation of the system in standard road vehicles, several issues should be addressed. First, we did not consider the impact of measurement errors that would take place in real conditions. Although there exist hardware and algorithms to compute all the inputs we used, they can be inaccurate or noisy in some circumstances. For example, it has been shown that the tangent point angle θ_{far} or TLC can be accurately computed in real-time imaging with a monocular in-vehicle camera, but errors in measurement increase beyond 35 m ahead of the vehicle [33], [34]. Concerning the vehicle dynamics, some measures are already available in standard vehicles (such as yaw rate and steering angle). However, to our knowledge, some states can be measured only with specific and expensive sensors, typically the slide slip angle, and their estimation is still an open problem (see, e.g., [35]) In all cases, it remains to be determined to what extent our shared control law is robust to such uncertainty in signal measurement.

In this paper, we have aimed at analyzing the stability of the assisted system with respect to the driver's variable behavior. The key point of this analysis was to answer the question as to whether the device should be adjusted to every driver, leading to more efforts on onboard driver model identification, or whether the device can cover a wide range of driving styles without needing individual adjustment. Still, further studies are needed to assess the potential benefits of adapting the control law to each driver.

Another open question is whether the driver parameters should be considered constant. The electronic co-pilot has been designed to be robust against the deviation of driver model parameters (see Section IV). However, the driver model parameters may be influenced by the behavior of advanced driver assistance system. It is not possible to answer this question yet, but the cybernetic model, together with the identification tools that we have proposed, should help to investigate this question.

Finally, human-factor experiments with a larger panel of participants and different driving conditions are required to further assess the developed assistance system. One central question currently under investigation concerns how to evaluate the quality of human–machine cooperation with various degrees of shared control, which could be achieved with our system by manipulating the cooperation criteria $\Gamma_a - \Gamma_d$. How the driver integrates the automation behavior into an internal model of the vehicle dynamics over time (medium-term and long-term adaptation) is also an important research question.

Appendix
Driver–Vehicle–Road Model Coefficients

$$a_{11c} = -\frac{2(c_j + c_r)}{MV_x}$$

$$a_{12c} = \frac{2(c_r l_r + c_f l_f)}{MV_x^2} - 1, \quad a_{15c} = \frac{2c_f}{MV_x R_s}$$

$$a_{21c} = \frac{2(c_r l_r - c_f l_f)}{J}$$

$$a_{22c} = \frac{2\left(c_r l_r^2 - c_f l_f^2\right)}{JV_x}, \quad a_{25c} = \frac{2c_f l_f}{JR_s}$$

$$a_{61c} = \frac{T_{S\beta}}{I_s}, \quad a_{62c} = \frac{T_{Sr}}{I_s}, \quad a_{65c} = -\frac{T_{S\beta}}{R_s I_s}$$

$$a_{66c} = -\frac{B_s}{I_s}, \quad c_r = c_{r0}\mu$$

$$c_f = c_{f0}\mu, \quad b_{61c} = \frac{1}{I_s}$$

$$T_{S\beta} = \frac{2K_p c_f \eta_t}{R_s}, \quad T_{Sr} = \frac{2K_p c_f \eta_t}{R_s}\frac{l_f}{V_x}$$

$$b_{12d} = \frac{1}{T_I}, \quad a_{11d} = -\frac{1}{T_I}$$

$$b_{22d} = -\frac{K_c}{V_x}\frac{2}{\tau_p}\frac{T}{T_I}, \quad a_{21d} = \frac{K}{V_x}\frac{2}{\tau_p}\left(\frac{T_L}{T_I} - 1\right)$$

$$a_{22d} = -\frac{2}{\tau_p}, \quad b_{n31d} = -b_{34d}T_{S\beta}$$

$$b_{n32d} = -b_{34d}T_{S\beta}\frac{l_f}{V_x}, \quad a_{33d} = -\frac{1}{T_N}$$

$$b_{32d} = \frac{K_r V_x + K_t}{T_N}\frac{K_c}{V_x}\frac{T_L}{T_I}$$

$$b_{n35d} = b_{33d} + \frac{T_{S\beta}}{R_S}b_{34d}, \quad b_{34d} = -\frac{1}{T_N}$$

$$a_{32d} = 2\frac{K_r V_x + K_t}{T_N},$$

$$a_{31d} = -\frac{K_r V_x + K_t}{T_N}\frac{K_c}{V_x}\left(\frac{T_L}{T_I} - 1\right)$$

$$b_{31d} = -K_p\frac{K_r V_x + K_t}{T_N}$$

$$b_{33d} = -\frac{K_t}{T_N}, \quad b_{21d} = \frac{2}{\tau_p}K_p.$$

REFERENCES

[1] W. G. Najm, J. D. Smith, and M. Yanagisawa, "Pre-crash scenario typology for crash avoidance research," Nat. Highway Transp. Safety Admin., Washington, DC, USA, Tech. Rep. DOT-HS-810 767, 2007.

[2] J. Navarro, F. Mars, and M. S. Young, "Lateral control assistance in car driving: Classification, review and future prospects," *IET Intell. Transp. Syst.*, vol. 5, no. 3, pp. 207–220, Sep. 2011.

[3] D. Abbink, M. Mulder, and E. Boer, "Haptic shared control: Smoothly shifting control authority?" *Cognit., Technol., Work*, vol. 14, no. 1, pp. 19–28, Mar. 2012.

[4] D. A. Abbink and M. Mulder, "Neuromuscular analysis as a guideline in designing shared control," in *Advances in Haptics*, M. H. Zadeh, Ed. New York, NY, USA: InTech, Apr. 2010, pp. 499–516.

[5] P. Griffiths and R. B. Gillespie, "Sharing control between humans and automation using haptic interface: Primary and secondary task performance benefits," *Hum. Factors*, vol. 47, no. 3, pp. 574–590, Fall 2005.

[6] M. Mulder, D. A. Abbink, and R. Boer, "The effect of haptic guidance on curve negotiation behaviour of young, experienced drivers," in *Proc. IEEE Syst. Man, Cybern. Conf.*, Singapore, Oct. 2008, pp. 804–809.

[7] K. H. Goodrich, P. Schutte, and R. Williams, "Piloted evaluation of the H-mode, a variable autonomy control system, in motion-based simulation," in *Proc. AIAA Atmos. Flight Mech. Conf.*, Honolulu, HI, USA, Aug. 2008, pp. 574–590.

[8] W. B. Griffin, W. R. Provancher, and M. R. Cutkosky, "Feedback strategies for telemanipulation with shared control of object handling forces," *Presence*, vol. 14, no. 6, pp. 720–731, Dec. 2005.

[9] D. Kragic, P. Marayong, M. Li, A. M. Okamura, and G. D. Hager, "Human–machine collaborative systems for microsurgical applications," *Int. J. Robot. Res.*, vol. 24, no. 9, pp. 731–741, 2005.

[10] C. Basdogan, A. Kiraz, I. Bukusoglu, A. Varol, and S. Doanay, "Haptic guidance for improved task performance in steering microparticles with optical tweezers," *Opt. Exp.*, vol. 15, no. 18, pp. 11616–11621, Sep. 2007.

[11] W. Mugge, D. A. Abbink, A. C. Schouten, J. P. A. Dewald, and F. C. T. Van der Helm, "A rigorous model of reflex function indicates that position and force feedback are flexibly tuned to position and force tasks," *Exp. Brain Res.*, vol. 200, no. 3/4, pp. 325–340, Jan. 2010.

[12] M. Mulder, M. M. R. van Paassen, and E. R. Boer, "Exploring the roles of information in the manual control of vehicular locomotion: From kinematics and dynamics to cybernetics," *Presence*, vol. 13, no. 5, pp. 535–548, Oct. 2004.

[13] F. Mars, L. Saleh, P. Chevrel, F. Claveau, and J. F. Lafay, "Modeling the visual and motor control of steering with an eye to shared-control automation," in *Proc. 55th Human Factors Ergon. Soc.*, Las Vegas, NV, USA, 2011, pp. 1422–1426.

[14] L. Saleh, P. Chevrel, F. Mars, J. F. Lafay, and F. Claveau, "Human-like cybernetic driver model for lane keeping," in *Proc. 18th IFAC World Congr.*, Milan, Italy, 2011, pp. 4368–4373.

[15] D. Salvucci and R. Gray, "A two-point visual control model of steering," *Perception*, vol. 33, no. 10, pp. 1233–1248, 2004.

[16] D. J. Cole, "Neuromuscular dynamics and steering feel," in *Proc. Steering Tech*, Munich, Germany, Mar. 2008. [Online]. Available: http://www2.eng.cam.ac.uk/~djc13/vehicledynamics/proj1.html

[17] A. Modjtahedzadeh and R. A. Hess, "A model of driver steering control behavior for use in assessing vehicle handling qualities," *Trans. ASME, J. Dyn. Syst. Meas. Control*, vol. 115, no. 3, pp. 456–464, Sep. 1993.

[18] C. Sentouh, P. Chevrel, F. Mars, and F. Claveau, "A sensorimotor driver model for steering control," in *Proc. IEEE Int. Conf. Syst., Man, Cybern.*, 2009, pp. 2462–2467.

[19] L. Ljung, *System Identification—Theory for the User*, 2nd ed. Upper Saddle River, N.J., USA: Prentice-Hall, 1999.

[20] L. Saleh, P. Chevrel, and J. F. Lafay, "Optimal control with preview for lateral steering of a passenger car: Design and test on a driving simulator," in *Time Delay Systems: Methods, Applications and New Trends*, R. Sipahi, T. Vyhlidal, S. I. Niculescu, and P. Pepe, Eds. Berlin, Germany: Springer-Verlag, Jan. 2012, pp. 173–185, Lect. Notes Contr. and Info. Sciences LNCIS.

[21] J. Godthelp, J. Milgram, and G. J. Blaauw, "The development of a time-related measure to describe driving strategy," *Hum. Factors*, vol. 26, no. 3, pp. 257–268, Jun. 1984.

[22] S. Mammar, S. Glaser, and M. Netto, "Time to line crossing for lane departure avoidance: A theoretical study and an experimental setting," *IEEE Trans. Intell. Transp. Syst.*, vol. 7, no. 2, pp. 226–241, Jun. 2006.

[23] L. Saleh, P. Chevrel, F. Claveau, J. F. Lafay, and F. Mars, "Contrôle latéral partagé d'un véhicule automobile: Conception à base d'un modèle cybernétique du conducteur et d'une commande H2 anticipative," *J. Eur. Syst. Autom.*, vol. 46, no. 4/5, pp. 535–557, 2012.

[24] G. Marro and E. Zattoni, "H2-optimal rejection with preview in the continuous-time domain," *Automatica*, vol. 41, no. 5, pp. 815–821, May 2005.

[25] A. Ferrante, G. Marro, and L. Ntogramatzidis, "A Hamiltonian approach to the H2 decoupling of previewed input signal," in *Proc. Eur. Control Conf.*, Kos, Greece, Jul. 2007, pp. 1149–1154.

[26] K. Zhou, J. C. Doyle, and K. Glover, *Robust and Optimal Control*. Upper Saddle River, NJ, USA: Prentice-Hall, 1996.

[27] W. F. Arnold and A. J. Laub, "Generalized eigenproblem algorithms and software for algebraic Riccati equations," *Proc. IEEE*, vol. 72, no. 12, pp. 1746–1754, Dec. 1984.

[28] J. Doyle, A. Packard, and K. Zhou, "Review of LFTs, LMIs and μ," in *Proc. 30th IEEE Conf. Decis. Control*, Brighton, U.K., 1991, pp. 1227–1232.

[29] P. Young and J. Doyle, "Computation of μ with real and complex uncertainties," in *Proc. 29th IEEE Conf. Decis. Control*, Honolulu, HI, USA, 1990, pp. 1230–1235.

[30] A. K. Packard, M. Fan, and J. Doyle, "A power method for the structured singular value," in *Proc. IEEE Conf. Decis. Control*, Austin, TX, USA, 1988, pp. 2132–2137.

[31] P. Young, M. Newlin, and J. Doyle, "Practical computation of the mixed μ problem," in *Proc. Amer. Control Conf.*, 1992, pp. 2190–2194.

[32] M. Fan, A. Tits, and J. Doyle, "Robustness in the presence of mixed parametric uncertainty and unmodeled dynamics," *IEEE Trans. Autom. Control*, vol. 36, no. 1, pp. 25–38, Jan. 1991.

[33] S. Glaser, R. Labayrade, S. Mammar, J. Douret, and B. Lusetti, "Validation of a vision based time to line crossing computation," in *Proc. IEEE Intell. Veh. Symp.*, Tokyo, Japan, 2006, pp. 200–205.

[34] R. Gallen and S. Glaser, "Vision based tangent point detection algorithm, evaluation and validation," in *Proc. IAPR Conf. Mach. Vis. Appl.*, Yokohama, Japan, 2009, pp. 518–521.

[35] J. Stephant, A. Charara, and D. Meizel, "Virtual sensor, application to vehicle sideslip angle and transversal forces," *IEEE Trans. Ind. Electron.*, vol. 51, no. 2, pp. 278–289, Apr. 2004.

Louay Saleh received the Engineer's degree in electronic systems from the Higher Institute of Applied Sciences and Technology, Damascus, Syria, in 2003 and the M.Sc. and Ph.D. degrees in automatic control from Ecole Centrale de Nantes, Nantes, France, in 2008 and 2012, respectively.

He is currently a Researcher with the Higher Institute of Applied Sciences and Technology. His research interests include system dynamics and control, with emphasis on mathematical modeling and control design, and control theory applied to autonomous systems.

Philippe Chevrel received the Ph.D. degree in automatic control from the University of Paris XI, Orsay, France, in 1993.

He is currently a Professor with Ecole des Mines de Nantes, Nantes, France, where he is responsible for the Department of Control Engineering and Production Systems. He is a member of the Control Team with the Research Institute of Communications and Cybernetics of Nantes (IRCCyN-UMR CNRS 6597), Ecole Centrale de Nantes. He is the author or co-author of more than 100 research publications and reports, including patents and chapters of books. His research interests include robust control, structured control and control implementation, and proper physical model, from theoretical to practical, with applications to automotive systems, power systems, vibration control, etc.

Fabien Claveau received the Engineer's degree from Ecole Nationale Supérieure d'Ingénieurs de Bourges, Bourges, France, in 2001 and the Ph.D. degree in automatic control from the University of Nantes and Ecole Centrale de Nantes, Nantes, France, in 2005.

Since 2005, he has been an Assistant Professor with the Ecole des Mines de Nantes and a member of the Control Team with Research Institute of Communications and Cybernetics of Nantes (IRCCyN-UMR CNRS 6597), Ecole Centrale de Nantes. His research interests include robust control, decentralized and distributed control design methodologies, and automotive engineering, particularly the design of driving assistance for conventional or more specific (e.g., narrow tilting) vehicles.

Jean-François Lafay received the Ph.D. degree and the Accreditation to Supervise Research from the University of Nantes, Nantes, France, in 1978 and 1985, respectively.

He is currently a Professor with Ecole Centrale de Nantes. He is also a member and former director (from 2000 to 2008) of the Control Team with the Research Institute of Communications and Cybernetics of Nantes (IRRCyN-CNRS), Ecole Centrale de Nantes. He is the author or co-author of more than 150 research publications and communications. His research interests include structural analysis and control of linear systems including (or not) time delays.

Dr. Lafay is a member of the Technical Committee on Linear Systems of the International Federation of Automatic Control.

Franck Mars received the M.Sc. degree in psychology from the University Charles de Gaulle, Lille, France, in 1997 and the Ph.D. degree in neuroscience from the University of Aix-Marseille 2, Marseille, France, in 2001.

After a one-year postdoctoral fellowship with Anatol Feldman's Motor Control Laboratory, University of Montreal, Montreal, QC, Canada, he joined the Research Institute of Communications and Cybernetics of Nantes (IRCCyN), Ecole Centrale de Nantes, Nantes, France, first as a Postdoctoral Fellow (from 2003 to 2004) and later as a permanent Full-Time Researcher. In 2012, he became the Group Head with the Psychology, Cognition, and Technology Group, IRCCyN. He favors an interdisciplinary approach at the crossroads of experimental psychology, ergonomics, and engineering sciences. His research interests include the design of technological systems based on the understanding of human behavior, with emphasis on perceptual and motor processes and how those processes interact with higher cognitive functions.

Dr. Mars is a member of the Human Factors and Ergonomics Society.